A variable temperature ultrahigh vacuum atomic force microscope

Q. Dai,[a] R. Vollmer,[b] R. W. Carpick,[c] D. F. Ogletree, and M. Salmeron
Materials Sciences Division, Lawrence Berkeley National Laboratory, Berkeley, California 94720

(Received 11 May 1995; accepted for publication 5 July 1995)

A new atomic force microscope (AFM) that operates in ultrahigh vacuum (UHV) is described. The sample is held fixed with spring clamps while the AMF cantilever and deflection sensor are scanned above it. Thus, the sample is easily coupled to a liquid nitrogen cooled thermal reservoir which allows AFM operation from ≈100 K to room temperature. AFM operation above room temperature is also possible. The microscope head is capable of coarse x-y positioning over millimeter distances so that AFM images can be taken virtually anywhere upon a macroscopic sample. The optical beam deflection scheme is used for detection, allowing simultaneous normal and lateral force measurements. The sample can be transferred from the AFM stage to a low energy electron diffraction/Auger electron spectrometer stage for surface analysis. Atomic lattice resolution AFM images taken in UHV are presented at 110, 296, and 430 K. © *1995 American Institute of Physics.*

I. INTRODUCTION

Since the development of the scanning tunneling microscope (STM), other "daughter" scanning probe microscopes have been introduced, including the atomic force microscope (AFM), which was first developed by Binning, Quate, and Gerber in 1986.[1] A small, sharp tip attached to the end of a small cantilever is brought close to and possibly in contact with the surface of a material and the resulting forces are measured.

One particular feature of AFM is that it allows the measurement of interaction forces due to adhesion and friction between tip and surface atoms. This opens up the possibility of studying these tribological phenomena at the atomic scale. In 1987, Mate *et al.* demonstrated the possibility of measuring atomic-scale frictional forces with the AFM.[2] They measured the lateral movement of the lever using optical interferometry. A tungsten tip was moved across a graphite sample with the normal load ranging from 7.5 to 56 μN. The authors observed lateral forces that varied with the atomic lattice periodicity during scanning. A linear dependence of frictional force on load was found. This result has since inspired others to further investigate tribological phenomena, namely contact, friction, and adhesion, on the atomic scale.

The majority of AFM studies so far have been performed in air or liquid. However this limits the range of materials that can be studied. In addition, true surface and tip cleanliness is nearly impossible to obtain in air. This is important, for example, because frictional forces crucially depend upon the experimental environment. Liquid films condensed around the tip from ambient vapor can act as a lubricant between the tip and sample, causing friction and adhesive forces to vary with changes in humidity.[3] The ideal conditions for surface science studies at the atomic level can only be achieved in ultrahigh vacuum (UHV). In this paper we present an AFM designed for variable temperature UHV operation. The instrument also allows sample introduction, as well as transfer from the AFM stage to a surface analysis stage with low energy electron diffraction (LEED) and Auger analysis capability. We will illustrate the performance of this instrument with images of NaCl, MoS_2, and mica cleaved in UHV.

The force detection scheme used for our instrument is the optical deflection method, developed by Meyer *et al.*[4] and Alexander *et al.*,[5] and improved by Marti *et al.*[6] In this detection scheme, a laser beam is reflected off the rear side of the cantilever and its deflection is measured by a position-sensing photodiode detector. Normal forces which bend the cantilever vertically, and lateral forces which twist the lever, can be independently and simultaneously measured.

As mentioned, most AFM results published so far have been performed in ambient conditions or liquid cell. The few UHV AFM systems developed so far operate only at room temperature[4,7–12] or additionally at liquid helium temperature.[13] Imaging at different temperatures, which is increasingly considered to be an important capability, is not easily performed with these other designs. To allow variable temperature operation, we have chosen to use the "walker" style microscope, based upon the scanning tunneling microscope design by Fröhn *et al.*[14] The key feature of the design is that the sample does not need to be attached to any piezoeletric elements for scanning or positioning. Instead, all the AFM components are mounted on a separate head supported by three piezo tubes. The light source (an optical fiber and lens), the cantilever, and the photodiode are scanned above the sample while the sample remains fixed. The sample resides in a sample holder that can then be easily clamped to a thermal reservoir for heating and cooling. This also allows easy sample transferring, as well as a large range of coarse tip positioning.

With the beam deflection scheme, the optical alignment is critical. Since vacuum operation restricts mechanical access to an experiment, and since the fine positioning required for optical alignment would considerably complicate the apparatus, we chose to do the optical alignment *ex situ*. We have found that optical misalignment after pumping and baking the chamber is small for Si levers,[15,16] as is thermal

[a]Current address: Aerodyne Research Inc., 45 Manning Rd. Billerica, MA 01821.
[b]Current address: Max-Planck-Institut für Mikrostrukturphysik, Weinberg 2, 06120 Halle/Saale, Germany.
[c]Also at Department of Physics, University of California at Berkeley.

 0034-6748/95/66(11)/5266/6/$6.00

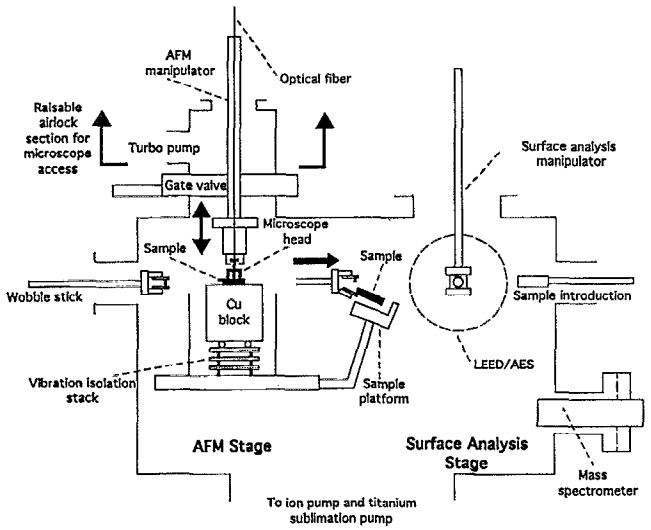

FIG. 1. Schematic representation of the major components of the UHV AFM chamber.

drift due to sample heating and cooling (to be discussed further in Sec. II C). Our system has an airlock to allow microscope access for occasional lever replacement or realignment without venting the whole UHV chamber. Details of our design will be described in Sec. II.

II. INSTRUMENTATION AND DESIGN

A. UHV system

A schematic drawing of the UHV-AFM system is shown in Fig. 1. The chamber consists of two stages: the AFM stage and the surface preparation/analysis stage. The sample is mounted in a sample holder which is transferred between these two stages with a wobble stick. The sample holder functions as an approach ramp for the microscope and will be described in Sec. II B. A load lock is included so that samples can be transferred in and out of the chamber without breaking vacuum. In addition, an airlock system above the AFM stage allows the microscope to be taken to air, to change cantilevers for instance, without breaking the vacuum inside the main chamber. The chamber is bolted onto a steel frame supported by four pneumatic isolators[17] to damp low frequency vibrations.

The surface preparation/analysis stage is equipped with conventional surface analysis techniques: an ion sputtering gun for sample cleaning, a quadrupole mass spectrometer, a gas doser, and a LEED/Auger electron spectrometer-optics system for sample preparation and characterization. The sample holder is clamped onto a manipulator. The sample is cooled by a liquid nitrogen cold finger which is connected to the manipulator with copper braids. The sample can also be heated through radiation and e-beam bombardment (for high temperature) by using a tungsten filament mounted within the sample manipulator. As such, the sample can be cooled below 100 K or heated above 2000 K.

The microscope head is attached to a second manipulator that can raise or lower the microscope over the AFM stage. The microscope can be raised through a gate valve to a five-

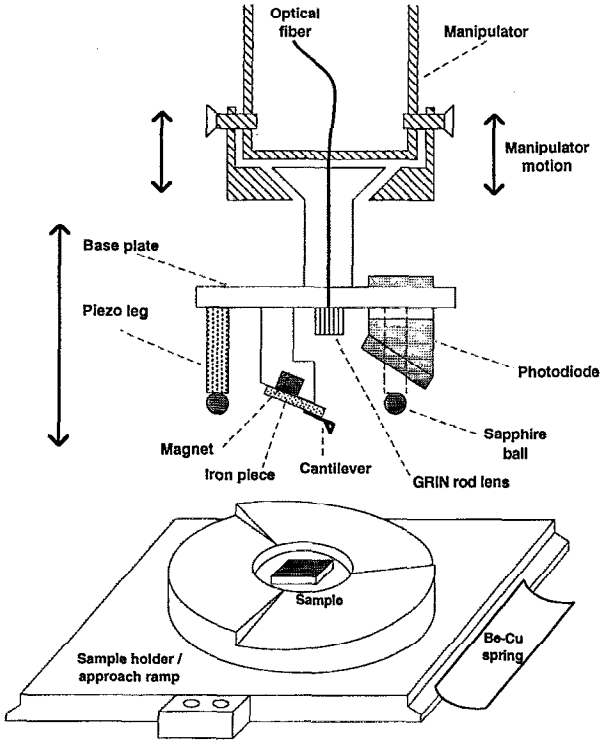

FIG. 2. Details of the UHV AFM head and the sample holder. Electrical connections to the photodiode and a piezo sectors are made with 0.003 in. wires running from a pin assembly above the manipulator (not shown). The iron piece and photodiode are positioned by hand for optical alignment.

way cross airlock system to allow microscope access (for cantilever replacement, etc.) without breaking the vacuum in the rest of the chamber. When the microscope is lowered onto the AFM sample stage, its three piezo tubes stand upon the sample holder, completely decoupled from the AFM manipulator (Fig. 2).

The sample holder is held onto a large Cu block, described below, with two Be–Cu foil springs so that it can be inserted and removed with the wobble stick, yet is sufficiently clamped to prevent vibrations and ensure good thermal contact. The cooling and heating of the sample will be discussed in Sec. II C.

The wobble stick is able to pick up and drop off a second sample from a platform located between the AFM and surface analysis stages. This allows a reference sample to be available at all times for immediate calibration and comparison.

The wobble stick can also be used to cleave samples *in situ*. We have designed a modified sample holder with a slot for a guided knife edge. Rapidly jerking the wobble stick forward while pushing on the knife edge provides enough force to cleave samples.

B. Microscope head arrangement

The microscope head and sample holder/approach ramp are depicted in Fig. 2. The microscope consists of a base plate, three piezo tubes for approaching and scanning, an optical fiber and lens, the cantilever, and a position-sensing photodiode detector. The Ni-plated aluminum base plate which holds all these elements is 1.25 in. in diameter and 0.1

in. thick. The three piezo tubes are located 120 degrees apart, on a 1-in.-diam circle. The mass of the microscope head should be kept small to maximize its stiffness. Since laser diodes require massive heat sinks during operation, it is not practical to attach to a laser diode directly to the microscope head. Furthermore, bakeout compatibility would involve nontrivial design considerations for the laser diode. We thus chose to bring light from an external laser diode into the chamber with a single-mode optical fiber. The fiber enters the chamber through a small hole drilled through a flange, sealed with Torr-Seal.[18] Outgassing from the fiber jacket in UHV is found to be negligible as the chamber base pressure is routinely below 5×10^{-10} Torr. Index-matching epoxy[19] attaches the fiber to a gradient index (GRIN) rod lens[20] on the microscope head which focuses the laser beam onto the cantilever.

We use commercially available microfabricated cantilevers which we attach to a small iron piece with low vapor pressure epoxy. The iron piece is in turn held onto the microscope by a magnet embedded in a central post as shown in Fig. 2. This allows easy positioning of the cantilever by moving the iron piece with tweezers so that the incident laser beam will be properly positioned at the center of the back end of the lever. The position of the laser spot is checked with an optical microscope. The end of the center post which contains the magnet is machined at a 22.5° angle, thus the reflected beam is at a 45° angle to the vertical incoming beam. With a Si or Si_3N_4 cantilever coated with gold, roughly 70% of the incident light is reflected off the back of the lever and collected by the photodiode.

The photodiode is mounted on an aluminum block, which is held onto the based plate with a thin Be–Cu foil which functions as a spring clamp. The position of the photodiode can be adjusted manually by moving the aluminum block within its slot until the beam is centered on the detector. The aluminum block is machined at a 45° degree angle so that the reflected laser beam will be normally incident, thus maintaining the original beam profile on the detector.

The microscope is supported by three piezo tubes 0.5 in. long, 120 degrees apart. They are used for offsetting, scanning, and inertial translation of the microscope. These tubes are 0.125 in. in diameter and have a wall thickness of 0.02 in. Sapphire balls are attached to their ends with low vapor pressure epoxy. The sapphire balls facilitate the inertial motion. The resulting static friction force is small enough to allow the sapphire balls to slide across the ramp when the voltage applied to the piezo is suddenly changed, but large enough to hold the microscope steady while it is being scanned.

The coarse approach mechanism is identical to that of the walker type STM.[14] A sawtooth voltage wave deforms the piezo legs in such a way that the microscope rotates through inertial motion. The sample holder, as illustrated in Fig. 2, consists of three sloped ramps machined along the circumference. Therefore, as the microscope head rotates, it slowly descends, approaching the tip toward the sample. The approach is halted when the lever makes contact with the sample. The microscope can be retracted by applying a reversed voltage signal so that the microscope will rotate up the ramp. Inertial motion can also translate the microscope laterally across the ramp to image different parts of the sample. The sample holder can accommodate a sample as large as 8×8 mm^2, all of which is accessible to the microscope.

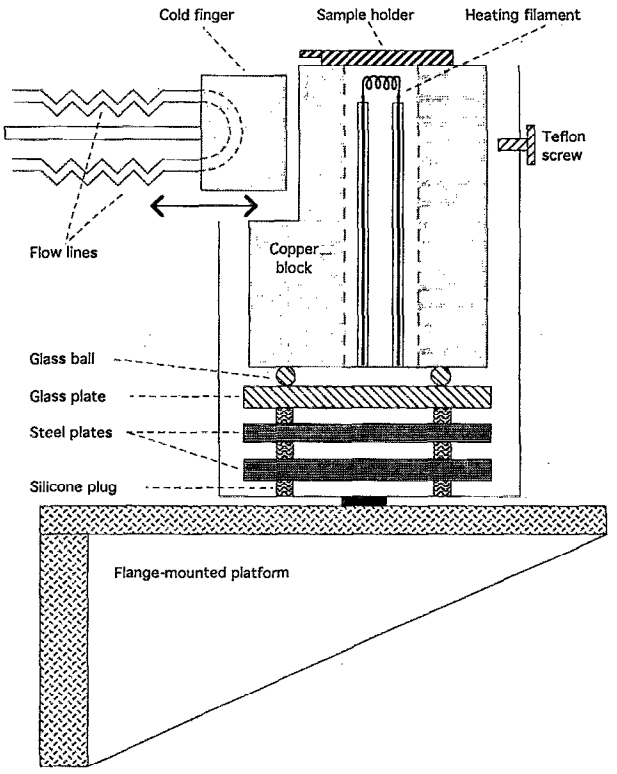

FIG. 3. Schematic representation of the AFM cryogenic arrangement.

The lowest eigenfrequency of the microscope head is ≈1.1 kHz. This limits the scan rate to less than 100 scan lines/s.

The microscope is controlled by RHK STM 100 electronics and a 486/33 PC. The photocurrents from the four segments of the quadrant detector are preamplified separately. These signals are then fed into a homemade electronics system which performs the summation and subtraction of the four signals.

C. Sample temperature variation at the AFM stage

Our method for sample temperature variation was designed primarily for AFM operation at or below room temperature, and so we will describe in detail the method and results of sample cooling. However, the AFM can also be operated with the sample substantially above room temperature.

The cryogenic arrangement is depicted in Fig. 3. The sample holder is mounted on top of a massive (≈3 kg) copper block, where it is held in place with two Be–Cu spring clamps. Under the copper block there is a stack which consists of two stainless steel plates with silicone rubber plugs in between for vibrational damping. The silicone[21] is preferable to Viton or other materials because it retains its elastic character over a large temperature range, and outgasses mini-

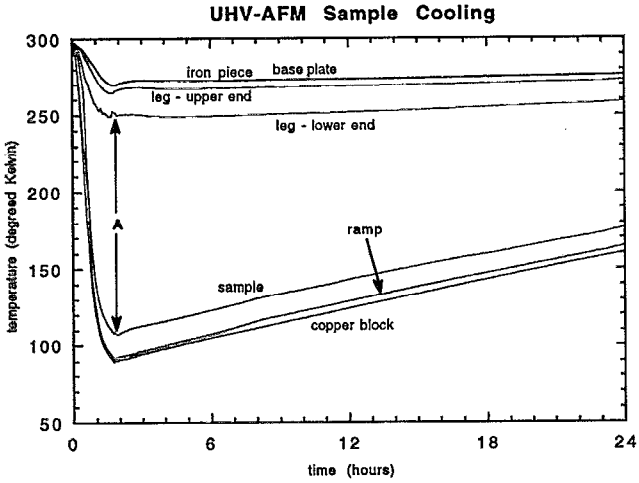

FIG. 4. Temperature vs time of the various AFM components below room temperature. A mica sample is mounted in the sample holder. At $t=0$, the cold finger is put in contact with the copper block. At point A ($t=1.5$ h), the cold finger is retracted. The mica sample has cooled to ≈105 K at this point. The initial warm-up rate is ≈3 K/h. Various parts of the microscope itself, including the low end of the piezo leg, do not cool substantially. The iron piece and microscope base plate curves nearly overlap.

mally. To reduce heat transfer, a glass plate separates the stack and copper block which sits on three 0.1-in.-diam glass balls. The copper block makes no other contact with the chamber.

The sample can be cooled with liquid nitrogen through a retractable cold finger to below 90 K. The cold finger is made of copper, with dimensions approximately 1 in.×1 in.×1 in., mounted on a linear motion feedthrough. Two thin-wall stainless steel tubes are welded onto the cold finger, connected via a hole machined through it to allow liquid nitrogen flow. The sample is cooled by flowing liquid nitrogen through the cold finger while it is pressed against the copper block. The cold finger is retracted once the sample has reached the desired temperature, leaving the sample and copper block mechanically isolated. The copper block is surrounded by a stainless steel shield which holds three Teflon set screws, set very close to but not in contact with the copper block to prevent it from tipping over when the cold finger is pressed against it.

To determine the temperatures of the various components of the AFM stage, thermocouples were attached to the copper block, the sample ramp, a mica sample, and four different parts of the microscope itself. The underside of the mica sample was attached to the sample holder with a thin layer of epoxy. Figure 4 shows the various temperatures plotted versus time. The first section of the plot is taken with the cold finger in contact with the copper block while liquid nitrogen is flowed through. The block cools down from room temperature to 90 K in less than 2 h. At point A, the cold finger is retracted and the copper block is now thermally and mechanically isolated. The components slowly warm up due to radiative heat transfer with their room temperature surroundings. The initial warming up rate of the sample is ≈3 K/h. This is slow enough to allow several images to be acquired within a one degree kelvin range. In this case, the sample remainged ≈15 degrees warmer than the sample holder due to the poor thermal conductivity of mica along its c axis. However the removable sample holder is only ≈2 degrees warmer than the copper block, showing that the spring clamping creates a good thermal contact between the sample holder and the copper block.

The lower end of one of the piezo legs of the microscope only cools to ≈250 K with the copper block at 90 K, indicating good thermal isolation. The upper part of the leg reaches a minimum temperature of ≈265 K. This demonstrates that over the entire low temperature range of the experiment, the peizo gain will not change dramatically. Indeed, by comparing atomic lattice resolution images taken at room temperature and at low temperature, we can measure the change in gain due to piezo cooling. With $T_{\text{block}}=100$ K, the gain was only about 10% smaller than at room temperature. This is consistent with the sensitivity decrease expected for piezos at approximately 250–260 K, according to the manufacturer's data. The microscope base and the iron piece which holds the cantilever both reach a minimum temperature of ≈270 K. Overall, we can conclude that the microscope is well insulated from the ramp.

All scanning probe microscopes are subject to some thermal drift. We measured the thermal drift with a Si cantilever[15] on a cooled mica sample in two separate experiments. In our case, roughly 60 min after the cold finger was retracted, with $T_{\text{block}}=100$ K, we measured thermal drift rates of typically 0.5–1 Å/s in the lateral direction and 0.2–0.4 Å/s in the z direction with the lever in a contact with the sample. These drift rates are not dramatically worse than the typical corresponding rates at 296 K: ≈0.3 Å/s or less laterally, ≈0.1 Å/s or less in z. Overall, the drift at 100 K is smooth and small enough so that it may be easily corrected for with image processing functions provided by the system software. The drift rates generally decreased with time as the microscope equilibrates further and the copper block warms up. Furthermore we expect the lever to cool somewhat due to radiative exchange with the sample. With the lever out of contact, we observed its equilibrium position drift upward by approximately 100 nm compared to room temperature. Despite this change in alignment, the laser spot has not deviated far enough from the center of the photodiode to impair deflection sensing. This upward bending of the lever is most likely due to the thin gold coating on the top of the lever which will undergo more thermal contraction upon cooling than the lever material itself (Si or Si_3N_4).[22] The lever relaxes to its original position when the AFM stage returns to room temperature.

Sample heating is conducted as follows. To temporarily heat the sample, a tungsten filament is mounted inside the copper block, shielded by a ceramic tube. The filament is buried inside ceramic shielding to reduce heat loss to the copper block, but is placed as close as possible to the sample to improve the heating efficiency. The sample can be heated to ≈500 K by radiation alone. However, to provide enough stability to acquire AFM images, the sample needs to be in thermal equilibrium with the copper block so that the rate of temperature decrease will be slow. To achieve this, the entire copper block can be heated; analogous to the cooling method, hot gas can be flowed through the retractable copper

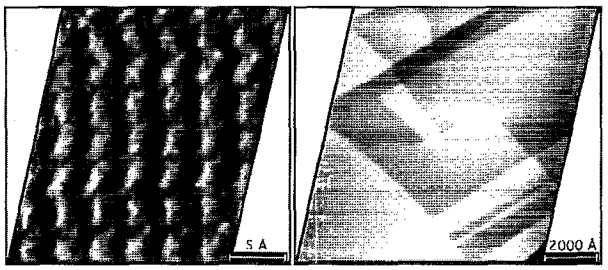

FIG. 5. Topographic images of NaCl(001) in UHV. (a) 30×30 Å^2 image showing atomic lattice resolution in UHV. The atomic corrugation is roughly 0.6 Å. The image was taken with an external loading force of ≈5 nN. (b) Large scale (1.2×1.2 μm^2) topographic image showing steps, as well as a screw dislocation in the upper left-hand part of the image. The nonrectangularity of the images is from a correction imposed to account for an asymmetric depolarization of the piezo tubes that was later improved.

block while it is in contact with the sample block to raise its temperature. If desired, one can simply take advantage of the elevated temperature of the copper block after baking the chamber. An image acquired in this fashion is presented in Sec. III.

III. EXPERIMENTAL RESULTS

All of the following results were acquired in UHV with a chamber pressure of 4×10^{-10} Torr or less using Si cantilevers[15] with a nominal spring constant of 1.1 N/m.

A. Imaging at room temperature

Figure 5 shows AFM images taken on a NaCl(001) surface, cleaved and imaged in UHV at room temperature in the topographic mode. Figure 5(a) is an atomic lattice resolution image of the NaCl(001) surface. The observed lattice spacing on NaCl(001) is 4.0±0.1 Å, matching well with the nearest-neighbor spacing between the individual ionic species (i.e., Cl^- ions) of 3.98 Å. Figure 5(b) is a large scale (1.4×1.4 μm) image, in which steps of monatomic and diatomic height are observed. A screw dislocation is also seen in he image.

B. Imaging above room temperature

Figure 6 shows a MoS_2 crystal cleaved in UHV and imaged at ≈430 K. In Fig. 6(a), the measured atomic periodicity is 3.1±0.1 Å, in agreement with nearest-neighbor separation of 3.16 Å. While performing this particular experiment, the character of the image changed dramatically at one point. Figure 6(b) shows an image that was subsequently obtained. The lattice is greatly distorted and the corrugation enhanced. We attribute this image to the presence of a sliding flake between the tip and the surface, a phenomenon previously observed with scanning probe microscopy on other layered materials.[23] The flake slides between the tip and sample during scanning, and the apparent lattice spacing along the scan direction is therefore reduced. By pulling the tip out of the contact with the surface and then placing it in contact again, the images reverted back to the type shown in Fig. 6(a), with the usual lattice spacing.

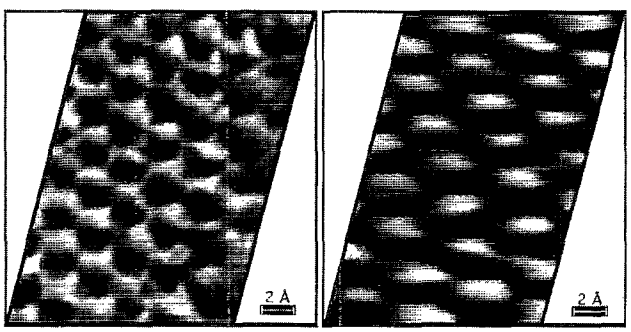

FIG. 6. Topographic images of MoS_2 at ≈430 K. (a) The usual lattice spacing (3.1 Å) is observed with weak (≈0.1 Å) corrugation. (b) A greatly distorted lattice and enhanced corrugation (≈0.8 Å) is temporarily imaged, possibly due to a sliding flake between the tip and surface. The nonrectangularity is explained in Fig. 5.

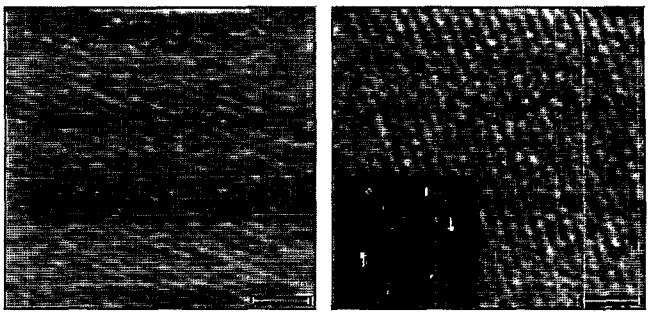

FIG. 7. Simultaneous topographic and lateral force images (100×100 Å^2) of mica at ≈110 K. The scale bar in the figures represents 20 Å. The topographic image possesses a streaked appearance along one of the lattice directions, while the lateral force image produced individual bumps for each lattice site. Contrast phenomena such as this are often observed with AFM images and are attributable to the nontrivial tip–surface interaction and unknown tip structure. Subsequent images showed clearer topographic contrast. The inset fast Fourier transform shows the expected symmetry for mica. The spot locations differ from those measured at room temperature by ≈10%, indicating a small decrease in piezo gain due to slight cooling. The spot angles (0°,56°,125°) indicate small distortion due to thermal drift during imaging. The images were acquired in approximately 30 s.

C. Imaging below room temperature

A mica sample was cleaved in UHV and then cooled until the sample block was at 90 K. A 100×100 Å atomic lattice resolution image is presented in Fig. 7, showing simultaneous topographic and lateral force images. This image was acquired roughly 60 min after lowering the microscope onto the cooled ramp/block. From the aforementioned temperature measurements, we estimate the sample temperature to be ≈110 K for this image. The inset spatial Fourier transform of the image indicates that distortion due to drift is not dramatic. The error in the spot position in the Fourier transform is due to a roughly 10% decrease in the piezo gain from slight cooling. We were able to reproducibly image the mica surface with atomic lattice resolution over the entire range of 110–296 K.

We subsequently introduced water vapor (triply distilled, then degassed with three freeze/pump/thaw cycles immediately before dosing) into the chamber through a leak valve with the sample cold (T_{block}=100 K). A 30 L exposure of water resulted in weakly bound structures that were dis-

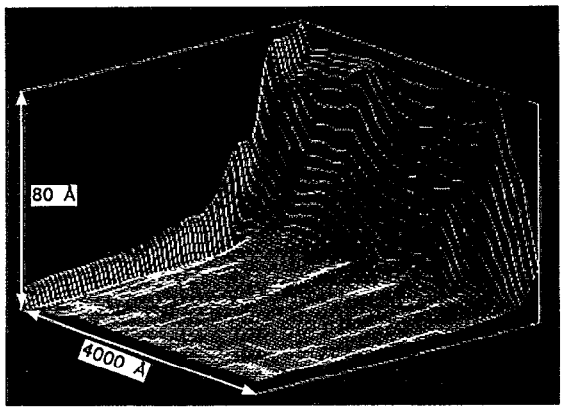

FIG. 8. Three-dimensional representation of repeated 4000 Å topographic line scans across a mica surface at ≈110 K after exposure to water. The first line scan reveals structures ~80 Å high which are worn away during each scan until a stable flat surface remains. The externally applied load during scanning was ≈1 nN.

rupted by the tip. Figure 8 shows a three-dimensional view of a topographic mode image where a 4000 Å line was repeatedly scanned (i.e., the microscope was not scanned along the slow-scan direction). About 80 Å of material was worn away by the tip during the first few line scans. This phenomenon was reproduced all over the sample. After a few scans, the atomic lattice of mica could be imaged. Only the usual mica surface was seen after the block temperature rose to ≈140 K. Further investigations of controlled water adsorption are in progress.

ACKNOWLEDGMENTS

We thank Professor N. Agraït of the Universidad Autonoma de Madrid who assisted with the mica experiments. This work was supported by the Director, Office of Energy Research, Basic Energy Sciences, Materials Division of the US Department of Energy under Contract No. DE-AC03-76SF00098. Q. D. acknowledges William Kolbe for many invaluable discussions. R.W.C. acknowledges the support of the Natural Sciences and Engineering Research Council of Canada.

[1] G. Binnig, C. F. Quate, and C. Gerber, Phys. Rev. Lett. **56**, 930 (1986).
[2] C. M. Mate, G. M. McClelland, R. Erlandsson, and S. Chiang, Phys. Rev. Lett. **59**, 1942 (1987).
[3] M. Binggeli and C. M. Mate, Appl. Phys. Lett. **65**, 415 (1994).
[4] G. Meyer and N. M. Amer, Appl. Phys. Lett. **56**, 2100 (1990).
[5] S. Alexander, L. Hellemans, O. Marti, J Schneir, V. Elings, P. K. Hansma, M. Longmire, and J. Gurley, J. Appl. Phys. **65**, 164 (1989).
[6] O. Marti, J. Colchero, and J. Mlynek, Nanotechnology **1**, 141 (1991).
[7] G. Neubauer, S. R. Cohen, G. M. McClelland, D. Horne, and C. M. Mate, Rev. Sci. Instrum. **61**, 2296 (1990).
[8] F. J. Germann, S. R. Cohen, G. Neubauer, G. M. McClelland, H. Seki, and D. Coulman, J. Appl. Phys. **73**, 163 (1993).
[9] L. Howald, E. Meyer, R. Lüthi, H. Haefke, R. Overney, H. Rudin, and H.-J. Güntherodt, Appl. Phys. Lett. **63**, 117 (1993).
[10] M. Kageshima, H. Yamada, K. Nakayama, H. Sakama, A. Kawau, T. Fujii, and M. Suzuki, J. Vac. Sci. Technol. B **11**, 1987 (1993).
[11] M. Ohta, Y. Sugawara, S. Morita, H. Nagaoka, S. Mishima, and T. Okada, J. Vac. Sci. Technol. B **12**, 1705 (1994).
[12] F. J. Giessibl and B. M. Trafas, Rev. Sci. Instrum. **65**, 1923 (1994).
[13] F. J. Giessibl, C. Gerber, and G. Binnig, J. Vac. Sci. Technol. B **9**, 984 (1991).
[14] J. Frohn, J. F. Wolf, K. Besocke, and M. Teske, Rev. Sci. Instrum. **60**, 1200 (1989).
[15] Ultralever, Park Scientific Instruments, Sunnyvale, CA.
[16] M. Radmacher, J. P. Cleveland, and P. K. Hansma, Scannings **17**, 117 (1995).
[17] Newport Corporation, Fountain Valley, CA.
[18] Varian Vacuum Products, Sugar Land, TX.
[19] Epoxy Technology Inc., Billerica, MA.
[20] NSG America Inc., Somerset, NJ.
[21] Parker Seals, Lexington, KY.
[22] O. Marti, A. Ruf, M. Hipp, H. Bielefeldt, J. Colchero, and J. Mlynek, Ultramicroscopy **42**, 345 (1992).
[23] M. Salmeron, D. F. Ogletree, C. Ocal, H.-C. Wang, G. Neubauer, W. Kolber, and G. Meyers, J. Vac. Sci. Technol. B **9**, 1347 (1991).